Molecular elucidation of brain lipofuscin in aging and Neuronal Ceroid Lipofuscinosis

Sofia Massaro Tieze[1,2], Alexander Esqueda,[1,2] Rachel McAllister,[3] Matija Lagator[4,5], Betül Yücel[1], Eric Sun[8], TuKiet T. Lam[6,7], Nicholas Lockyer[4], Kallol Gupta[3], Sreeganga S. Chandra[1,9,10,*]

[1]Departments of Neurology & Neuroscience, Yale University, New Haven, CT, USA
[2]Interdepartmental Neuroscience Program, Yale University, New Haven, CT, USA
[3]Department of Cell Biology, Yale University, New Haven, CT, USA
[4]Photon Science Institute, Department of Chemistry, University of Manchester, Manchester, UK
[5]Rosalind Franklin Institute, Rutherford Appleton Laboratory, Didcot, Oxfordshire, UK
[6]Departments of Molecular Biophysics and Biochemistry, Yale University, New Haven, CT, USA
[7]Keck Mass Spectrometry & Proteomics Resource, W.M. Keck Biotechnology Resource Laboratory, New Haven, CT, USA
[8]Yale College, Yale University, New Haven, CT, USA
[9]Senior author
[10]Lead contact
*Correspondence: sreeganga.chandra@yale.edu

SUPPLEMENTAL FIGURES

Fig. S1.

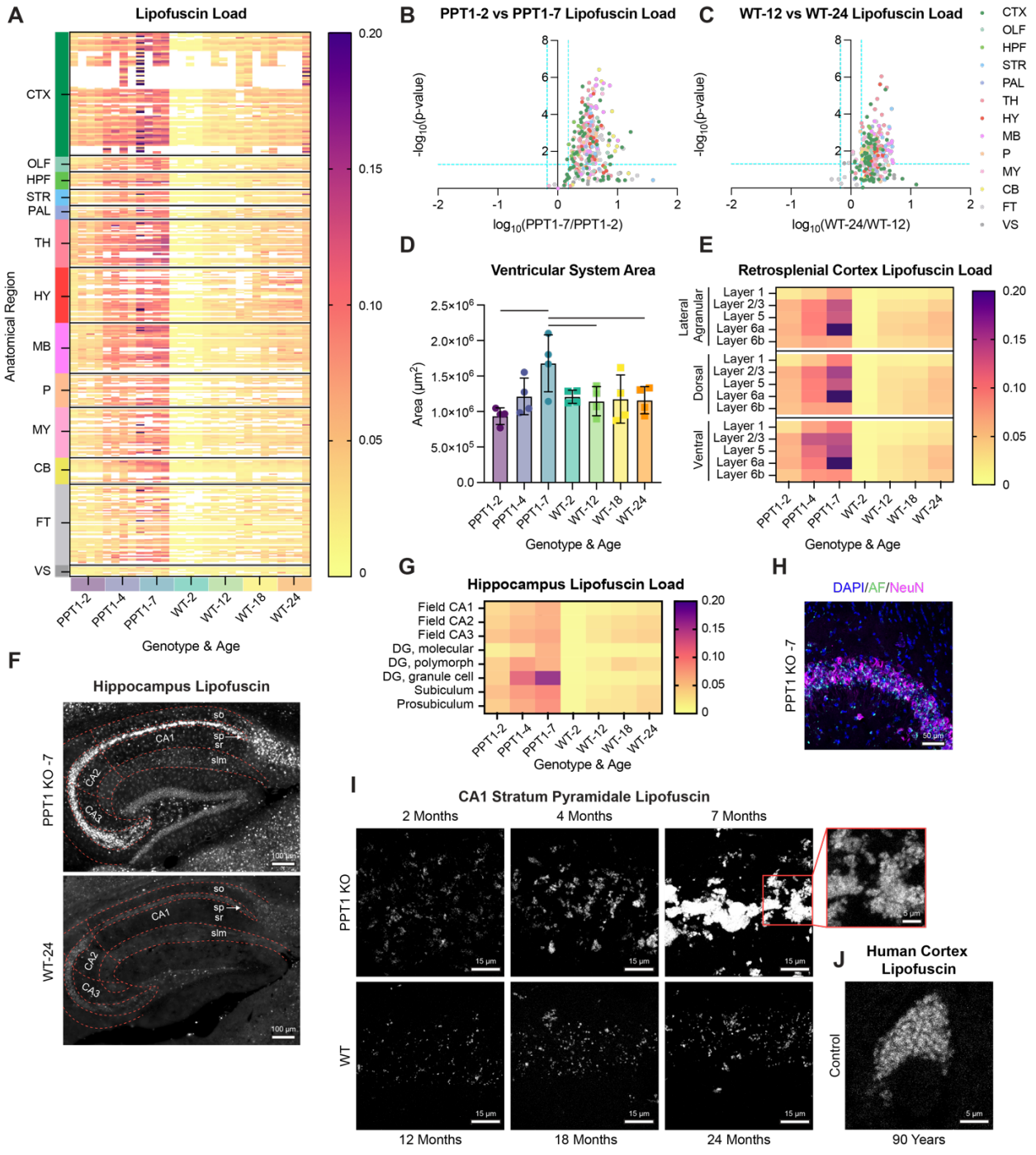
A
Lipofuscin Load
Anatomical Region
CTX
OLF
HPF
STR
PAL
TH
HY
MB
P
MY
CB
FT
VS
PPT1-2
PPT1-4
PPT1-7
WT-2
WT-12
WT-18
WT-24
Genotype & Age
0.20
0.15
0.10
0.05
0
B
PPT1-2 vs PPT1-7 Lipofuscin Load
-log10(p-value)
log10(PPT1-7/PPT1-2)
C
WT-12 vs WT-24 Lipofuscin Load
log10(WT-24/WT-12)
D
Ventricular System Area
Area (μm²)
E
Retrosplenial Cortex Lipofuscin Load
Lateral Agranular
Dorsal
Ventral
Layer 1
Layer 2/3
Layer 5
Layer 6a
Layer 6b
F
Hippocampus Lipofuscin
PPT1 KO -7
WT-24
so
sp
sr
slm
CA1
CA2
CA3
100 μm
G
Hippocampus Lipofuscin Load
Field CA1
Field CA2
Field CA3
DG, molecular
DG, polymorph
DG, granule cell
Subiculum
Prosubiculum
H
DAPI/AF/NeuN
PPT1 KO -7
50 μm
I
CA1 Stratum Pyramidale Lipofuscin
2 Months
4 Months
7 Months
PPT1 KO
WT
12 Months
18 Months
24 Months
15 μm
5 μm
J
Human Cortex Lipofuscin
Control
90 Years

Figure S1. Lipofuscin load increases across fine neuroanatomical regions with age and *CLN1* progression.

(**A**) Heat map of lipofuscin load across fine anatomical regions (n = 4 sex-matched biological replicates/genotype/timepoint; n = 4 alternate sections/replicate). White cells indicate that region was not found in measured sections. Rows corresponding to regions with fewer than 2 measurements across all samples were not included. Color blocks on left correspond to location of region within Allen Mouse Brain Atlas as in **Fig. 1Biv** (CTX: isocortex; OLF: olfactory areas; HPF: hippocampal formation; STR: striatum; PAL: pallidum; TH: thalamus; HY: hypothalamus; MB: midbrain; P: pons; MY: medulla; CB: cerebellum; FT: fiber tracts; VS: ventricular systems). Color blocks on bottom correspond to age and genotype of animals as in **Fig. 1A**.

(**B** and **C**) Log fold-change comparisons of lipofuscin load by fine (points) and gross (color groups) anatomical regions with (B) *CLN1* progression in 2- vs 7-month-old PPT1 KO mice and with (C) natural aging in 12- vs. 24-month-old WT mice (blue dashed line significance threshold at fold change > 1.5 and $p < 0.05$).

(**D**) Quantification of ventricular system area (μm^2) with age and *CLN1* progression (n = 4 sex-matched biological replicates/genotype/timepoint; n = 4 alternate sections/biological replicate). Lines indicate statistical comparisons where $p < 0.05$ by Tukey's multiple comparison test.

(**E**) Heat map of lipofuscin load in lateral agranular (top) and dorsal (middle) and ventral (bottom) retrosplenial areas by cortical layer (average of n = 4 sex-matched biological replicates/genotype/timepoint; n = 4 alternate sections/replicate).

(**F**) Representative images of hippocampus autofluorescence in PPT1 KO 7-month (top) and WT 24-month (bottom) animals (scale bar, 100 μm). Red dashed lines indicate fine anatomical regions of fields CA1, CA2 and CA3 (so: *stratum oriens*; sp: *stratum pyramidale*; sr: *stratum radiatum*; slm: *stratum lacunosum-moleculare*).

(**G**) Heat map of lipofuscin load in hippocampal formation regions. Fields CA1, CA2, CA3 are averaged across fine regions shown in panel F (DG: dentate gyrus; average of n = 4 sex-matched biological replicates/genotype/timepoint; n = 4 alternate sections/replicate).

(**H**) PPT1 KO 7-month hippocampus *stratum pyramidale* with lipofuscin autofluorescence (AF; green), counterstained with nuclear marker DAPI (blue), and neuronal marker NeuN (magenta) (scale bar, 50 μm).

(**I**) Representative 63X images illustrating accumulation of autofluorescent lipofuscin granules in cells of *stratum pyramidale* layer of CA1 of hippocampus in PPT1 KO and WT mice with *CLN1* progression and age (scale bar, 15 μm). Inset shows region in red box at lower brightness to illustrate individual granules in saturated areas (scale bar, 5 μm).

(**J**) Representative lipofuscin-positive cell of dorsolateral prefrontal cortex of elderly human control (age = 90 years).

Fig. S2.

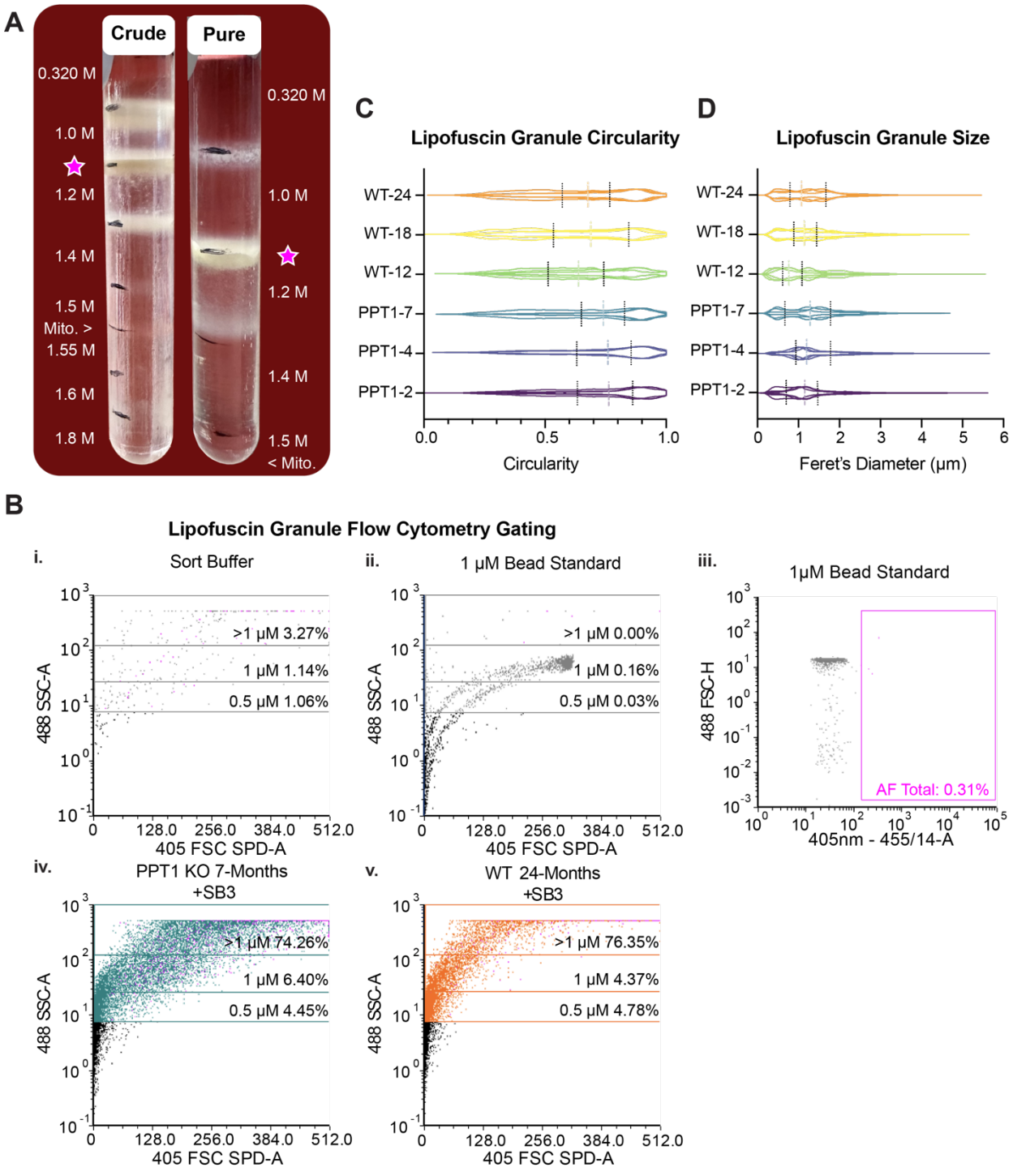
A
Crude
Pure
0.320 M
1.0 M
1.2 M
1.4 M
1.5 M
Mito. >
1.55 M
1.6 M
1.8 M
0.320 M
1.0 M
1.2 M
1.4 M
1.5 M
< Mito.
C
Lipofuscin Granule Circularity
WT-24
WT-18
WT-12
PPT1-7
PPT1-4
PPT1-2
0.0
0.5
1.0
Circularity
D
Lipofuscin Granule Size
WT-24
WT-18
WT-12
PPT1-7
PPT1-4
PPT1-2
0
1
2
3
4
5
6
Feret's Diameter (µm)
B
Lipofuscin Granule Flow Cytometry Gating
i.
Sort Buffer
>1 µM 3.27%
1 µM 1.14%
0.5 µM 1.06%
488 SSC-A
405 FSC SPD-A
ii.
1 µM Bead Standard
>1 µM 0.00%
1 µM 0.16%
0.5 µM 0.03%
488 SSC-A
405 FSC SPD-A
iii.
1µM Bead Standard
AF Total: 0.31%
488 FSC-H
405nm - 455/14-A
iv.
PPT1 KO 7-Months
+SB3
>1 µM 74.26%
1 µM 6.40%
0.5 µM 4.45%
488 SSC-A
405 FSC SPD-A
v.
WT 24-Months
+SB3
>1 µM 76.35%
1 µM 4.37%
0.5 µM 4.78%
488 SSC-A
405 FSC SPD-A

Figure S2. Lipofuscin purification and flow-cytometry strategies.

(**A**) Representative images of crude (left) and pure (right) sucrose gradients following ultracentrifugation. Yellow-brown autofluorescent fraction at 1.0-1.2 M sucrose interface is denoted by purple star. "Mito." indicates density at which healthy mitochondria sediment.

(**B**) Flow cytometry gating plots of (**i**) sort buffer control, (**ii**) 1 μm plastic size-standard beads for small-particle gating, (**iii**) 1 μm plastic size-standard beads approximating lipofuscin granule size excluded by autofluorescence gate, and SB3-stained lipofuscin from (**iv**) PPT1 KO 7-month and (**v**) WT 24-month animals illustrating majority of particles falling above 1 μm in diameter.

(**C-D**) Quantification of bright field SB3-stained granule images for (C) particle circularity and (D) particle size (Feret's Diameter) ($n = 3$ biological replicates/genotype/age; $n = 5$ images/replicate). Solid lines = 25th and 75th percentile and dashed lines = median for summed replicate data.

Fig. S3.

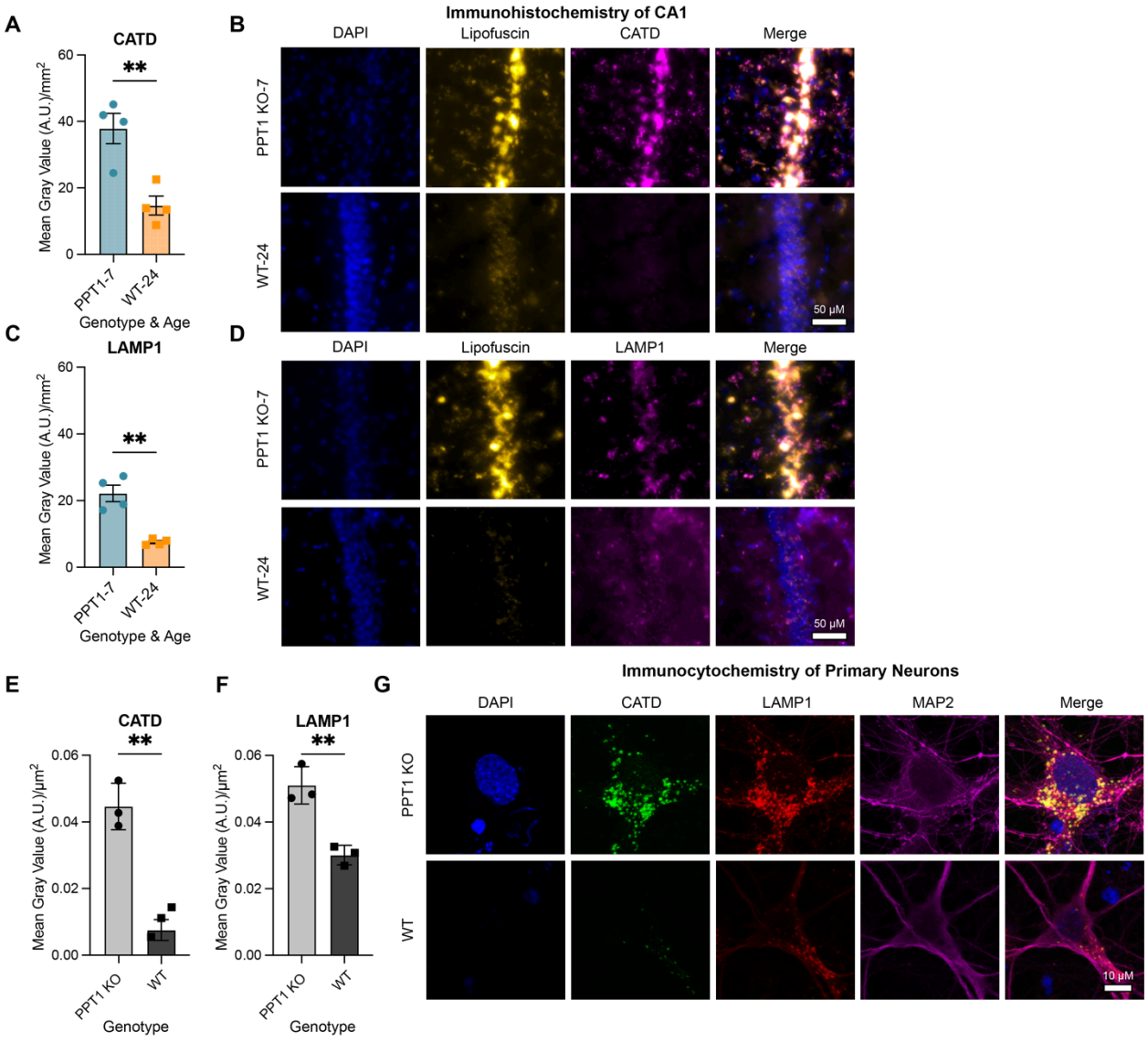
A
CATD
**
Mean Gray Value (A.U.)/mm²
60
40
20
0
PPT1-7
WT-24
Genotype & Age
B
Immunohistochemistry of CA1
DAPI
Lipofuscin
CATD
Merge
PPT1 KO-7
WT-24
50 µM
C
LAMP1
**
Mean Gray Value (A.U.)/mm²
60
40
20
0
PPT1-7
WT-24
Genotype & Age
D
DAPI
Lipofuscin
LAMP1
Merge
PPT1 KO-7
WT-24
50 µM
E
CATD
**
Mean Gray Value (A.U.)/µm²
0.06
0.04
0.02
0.00
PPT1 KO
WT
Genotype
F
LAMP1
**
Mean Gray Value (A.U.)/µm²
0.06
0.04
0.02
0.00
PPT1 KO
WT
Genotype
G
Immunocytochemistry of Primary Neurons
DAPI
CATD
LAMP1
MAP2
Merge
PPT1 KO
WT
10 µM

Figure S3. PPT1 KO results in lysosome accumulation.

(**A**) Quantification of cathepsin D (CATD) expression (mean gray value/mm^2) in hippocampal formation of 7-month PPT1 KO and 24-month WT mice. Data are mean ± SD of $n = 4$ sex-matched biological replicates; $n = 4$ sections/replicate.

(**B**) Representative images of lipofuscin autofluorescence (yellow) and CATD expression (magenta) in CA1 *stratum pyramidale* layer of hippocampus in 7-month PPT1 KO and 24-month WT mice with DAPI counterstain (blue) (scale bars, 50 μm).

(**C**) Quantification of LAMP1 lysosomal marker expression (mean gray value/mm^2) in the hippocampal formation of 7-month PPT1 KO and 24-month WT mice. Data are mean ± SD of $n = 4$ sex-matched biological replicates; $n = 4$ sections/replicate.

(**D**) Representative images of lipofuscin autofluorescence (yellow) and LAMP1 expression (magenta) in CA1 *stratum pyramidale* layer of hippocampus in 7-month PPT1 KO and 24-month WT mice with DAPI counterstain (blue) (scale bars, 50 μm).

(**E-F**) Quantification of (E) CATD and (F) LAMP1 expression (mean gray value/mm^2) in MAP2 positive neurons (magenta) in PPT1 KO and WT primary cortical cultures at DIV14. Data are mean ± SD of $n = 3$ independent cultures; $n = 5$ neurons/culture.

(**G**) Representative images of CATD (green) and LAMP1 expression (red) in MAP2 positive neurons (magenta) with DAPI counterstain (blue) in PPT1 KO and WT primary cortical cultures at DIV14 (scale bars, 10 μm).

Fig. S4.

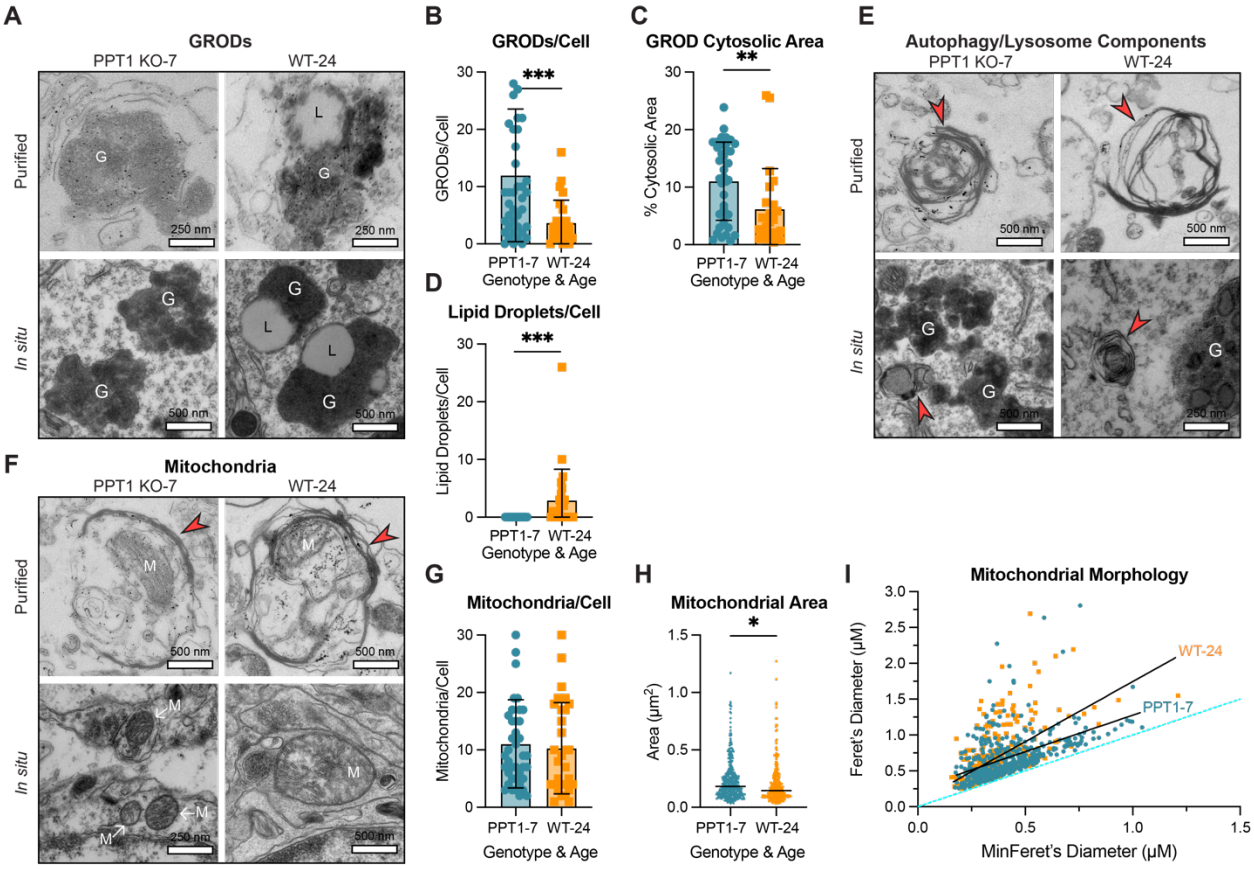
A
GRODs
PPT1 KO-7
WT-24
Purified
In situ
G
L
250 nm
500 nm
B
GRODs/Cell
***
GRODs/Cell
PPT1-7 WT-24
Genotype & Age
C
GROD Cytosolic Area
**
% Cytosolic Area
D
Lipid Droplets/Cell
***
Lipid Droplets/Cell
E
Autophagy/Lysosome Components
F
Mitochondria
M
G
Mitochondria/Cell
H
Mitochondrial Area
*
Area (μm²)
I
Mitochondrial Morphology
WT-24
PPT1-7
Feret's Diameter (μM)
MinFeret's Diameter (μM)

Figure S4. Ultrastructure of *in situ* and purified lipofuscin.

(**A**) Additional representative electron micrographs of granular osmiophilic deposit (GROD) structures (G) with associated lipid droplets (L) in purified lipofuscin (top) and *in situ* in PPT1 KO 7-month and WT 24-month brain (bottom) (scale bars, 250 or 500 nm).

(**B**) Quantification of electron micrographs of cytosolic GROD structures / cell in PPT1 KO 7-month and WT 24-month motor cortex and CA3 of hippocampus (*** indicates $p < 0.001$ by two-tailed t-test; WT: $n = 26$ cells; PPT1 KO: $n = 41$ cells).

(**C**) Quantification of percentage (%) of cytosolic area taken up by GROD structures in PPT1 KO 7-month and WT 24-month motor cortex and CA3 of hippocampus (** indicates $p < 0.01$ by two-tailed t-test; WT: $n = 26$ cells; PPT1 KO: $n = 41$ cells).

(**D**) Quantification of number of lipid droplets per cell in PPT1 KO 7-month and WT 24-month motor cortex and CA3 of hippocampus (*** $p < 0.001$ by two-tailed t-test; WT: $n = 26$ cells; PPT1 KO: $n = 41$ cells).

(**E**) Additional representative electron micrographs of putative multilamellar lysosomes (red arrowheads) in purified autofluorescent fractions (top) and PPT1 KO 7-month and WT 24-month brain (bottom) (scale bars, 250 nm or 500 nm; G, GROD).

(**F**) Representative electron micrographs of mitochondria (M) with disordered, sparse, or degraded cristae in putative multilamellar lysosome structures (red arrows) in purified autofluorescent fraction (top) or near synaptic densities in PPT1 KO 7-month and WT 24-month brain (bottom) (scale bars, 250 or 500 nm).

(**G**) Quantification of mitochondrial number per cell soma in PPT1 KO 7-month and WT 24-month motor cortex and CA3 of hippocampus (not significant by two-tailed t-test; WT: $n = 30$ cells; PPT1 KO: $n = 40$ cells).

(**H**) Quantification of mitochondrial area in the soma of cells in PPT1 KO 7-month and WT 24-month motor cortex and CA3 of hippocampus (* $p < 0.05$ by unpaired two-tailed t-test; WT: $n = 309$ mitochondria; PPT1 KO: $n = 447$ mitochondria).

(**I**) Simple linear regression of Feret's diameter (maximum caliper) versus minFeret's diameter (minimum caliper) of mitochondria in PPT1 KO 7-month and WT 24-month motor cortex and CA3 of hippocampus (PPT1-7: $y = 1.018*X + 0.2587$; $R^2 = 0.2582$; WT-24: $Y = 1.675*X + 0.07064$; $R^2 = 0.3524$; $p < 0.0001$ by F-test; WT: $n = 309$ mitochondria; PPT1 KO: $n = 447$ mitochondria). Blue dashed line represents perfect circularity ($Y = 1*X$).

Fig. S5.

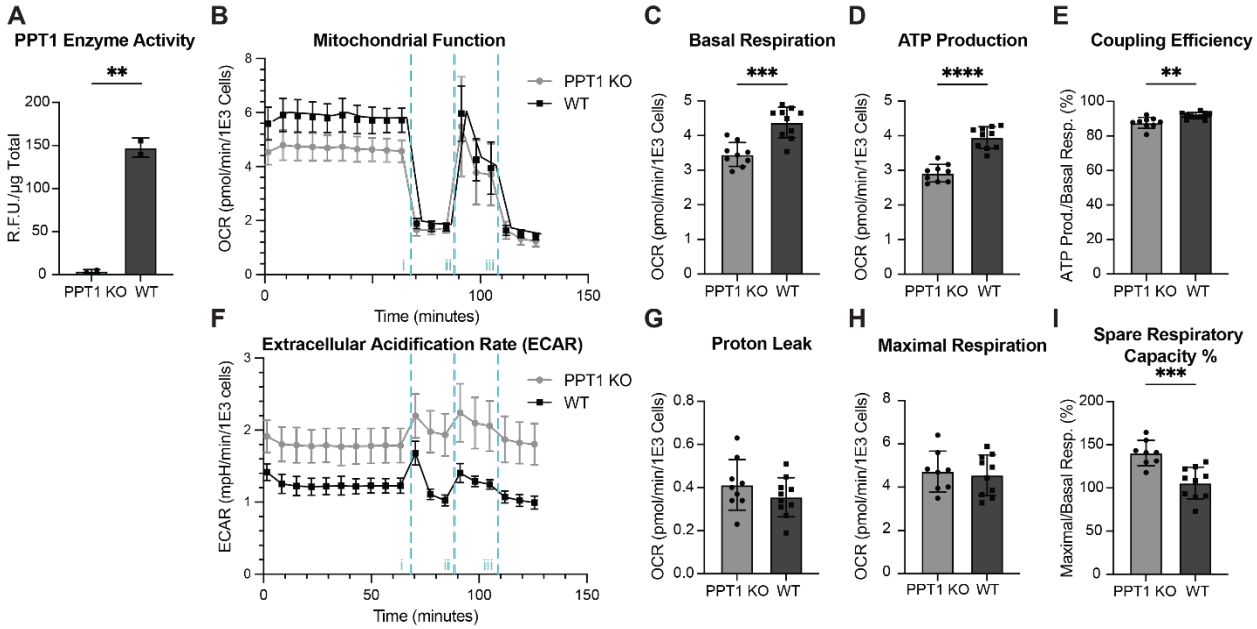
A
PPT1 Enzyme Activity
**
R.F.U./µg Total
PPT1 KO
WT
B
Mitochondrial Function
OCR (pmol/min/1E3 Cells)
PPT1 KO
WT
Time (minutes)
C
Basal Respiration
***
D
ATP Production
****
E
Coupling Efficiency
**
ATP Prod./Basal Resp. (%)
F
Extracellular Acidification Rate (ECAR)
ECAR (mpH/min/1E3 cells)
G
Proton Leak
H
Maximal Respiration
I
Spare Respiratory Capacity %
***
Maximal/Basal Resp. (%)

Figure S5. PPT1 KO causes aberrant mitochondrial flux.

(**A**) PPT1 enzyme activity in CRISPR-engineered HEK293T PPT1 KO cells and WT controls normalized to protein concentration (μg) determined by BCA ($n = 2$ independent cultures).

(**B**) Mitochondrial stress test with nutrient-deprivation performed on control (WT) and CRISPR-engineered PPT1 KO HEK293T cells, with sequential injections of mitochondrial inhibitors, (i) oligomycin A, (ii) FCCP, and (iii) rotenone/antimycin A (represented by vertical blue dashed lines), to determine effects on oxygen consumption rate (OCR). OCR measurements are normalized to cell number (per thousand cells) in each well. Parameters calculated from this metabolic flux signature are shown in the following panels.

(**C**) Basal respiration.

(**D**) ATP production.

(**E**) Coupling efficiency percent (%) (ATP production/basal respiration).

(**F**) Extracellular acidification rate (ECAR) with mitochondrial inhibitor injections as in panel A.

(**G**) Proton leak.

(**H**) Maximal respiration.

(**I**) Percentage of spare respiratory capacity (%) (maximal respiration/basal respiration). Data are mean ± SD. * $p < 0.05$, ** $p < 0.01$, *** $p < 0.001$, **** $p < 0.0001$ by unpaired two-tailed t-test. Data shown are representative results from one of two independent experiments (n = 9-10 replicate wells/genotype).

Fig. S6.

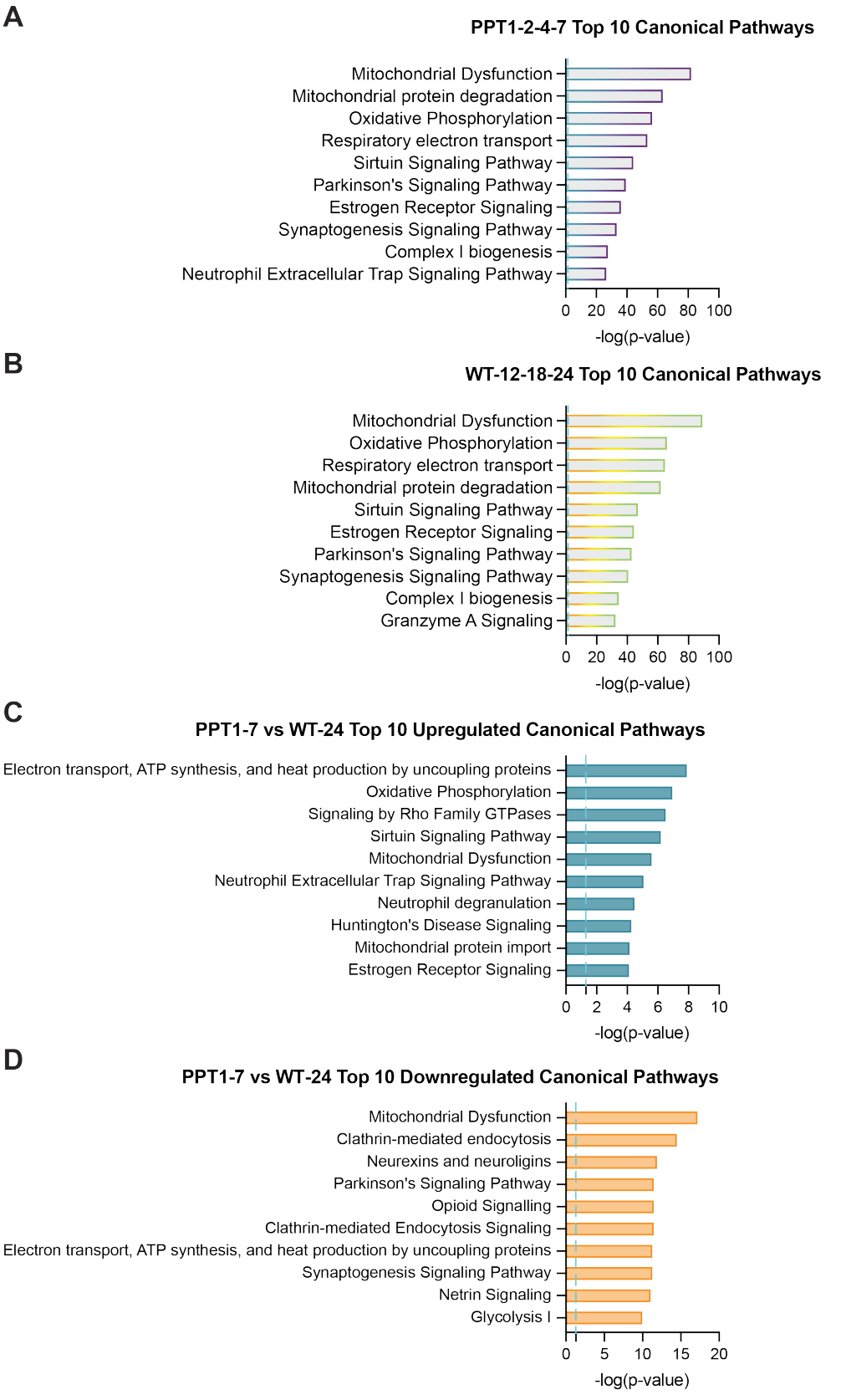
A
PPT1-2-4-7 Top 10 Canonical Pathways
Mitochondrial Dysfunction
Mitochondrial protein degradation
Oxidative Phosphorylation
Respiratory electron transport
Sirtuin Signaling Pathway
Parkinson's Signaling Pathway
Estrogen Receptor Signaling
Synaptogenesis Signaling Pathway
Complex I biogenesis
Neutrophil Extracellular Trap Signaling Pathway
0 20 40 60 80 100
-log(p-value)
B
WT-12-18-24 Top 10 Canonical Pathways
Mitochondrial Dysfunction
Oxidative Phosphorylation
Respiratory electron transport
Mitochondrial protein degradation
Sirtuin Signaling Pathway
Estrogen Receptor Signaling
Parkinson's Signaling Pathway
Synaptogenesis Signaling Pathway
Complex I biogenesis
Granzyme A Signaling
0 20 40 60 80 100
-log(p-value)
C
PPT1-7 vs WT-24 Top 10 Upregulated Canonical Pathways
Electron transport, ATP synthesis, and heat production by uncoupling proteins
Oxidative Phosphorylation
Signaling by Rho Family GTPases
Sirtuin Signaling Pathway
Mitochondrial Dysfunction
Neutrophil Extracellular Trap Signaling Pathway
Neutrophil degranulation
Huntington's Disease Signaling
Mitochondrial protein import
Estrogen Receptor Signaling
0 2 4 6 8 10
-log(p-value)
D
PPT1-7 vs WT-24 Top 10 Downregulated Canonical Pathways
Mitochondrial Dysfunction
Clathrin-mediated endocytosis
Neurexins and neuroligins
Parkinson's Signaling Pathway
Opioid Signalling
Clathrin-mediated Endocytosis Signaling
Electron transport, ATP synthesis, and heat production by uncoupling proteins
Synaptogenesis Signaling Pathway
Netrin Signaling
Glycolysis I
0 5 10 15 20
-log(p-value)

Figure S6. Ingenuity Pathway Analysis (IPA) of lipofuscin proteins.

Top 10 canonical pathways by Ingenuity Pathway Analysis of:

(**A**) Consensus PPT1 KO lipofuscin proteins across timepoints ($n = 745$) (**Fig. 3A**).

(**B**) Consensus WT lipofuscin proteins across timepoints ($n = 957$) (**Fig. 3A**).

(**C**) Significantly upregulated lipofuscin proteins in PPT1 KO 7-month/WT 24-month samples ($n = 83$) (**Fig. 3N**).

(**D**) Significantly downregulated lipofuscin proteins in PPT1 KO 7-month/WT 24-month samples ($n = 348$) (**Fig. 3N**).

Blue dashed line indicates significance threshold at $p = 0.05$, throughout.

Fig. S7.

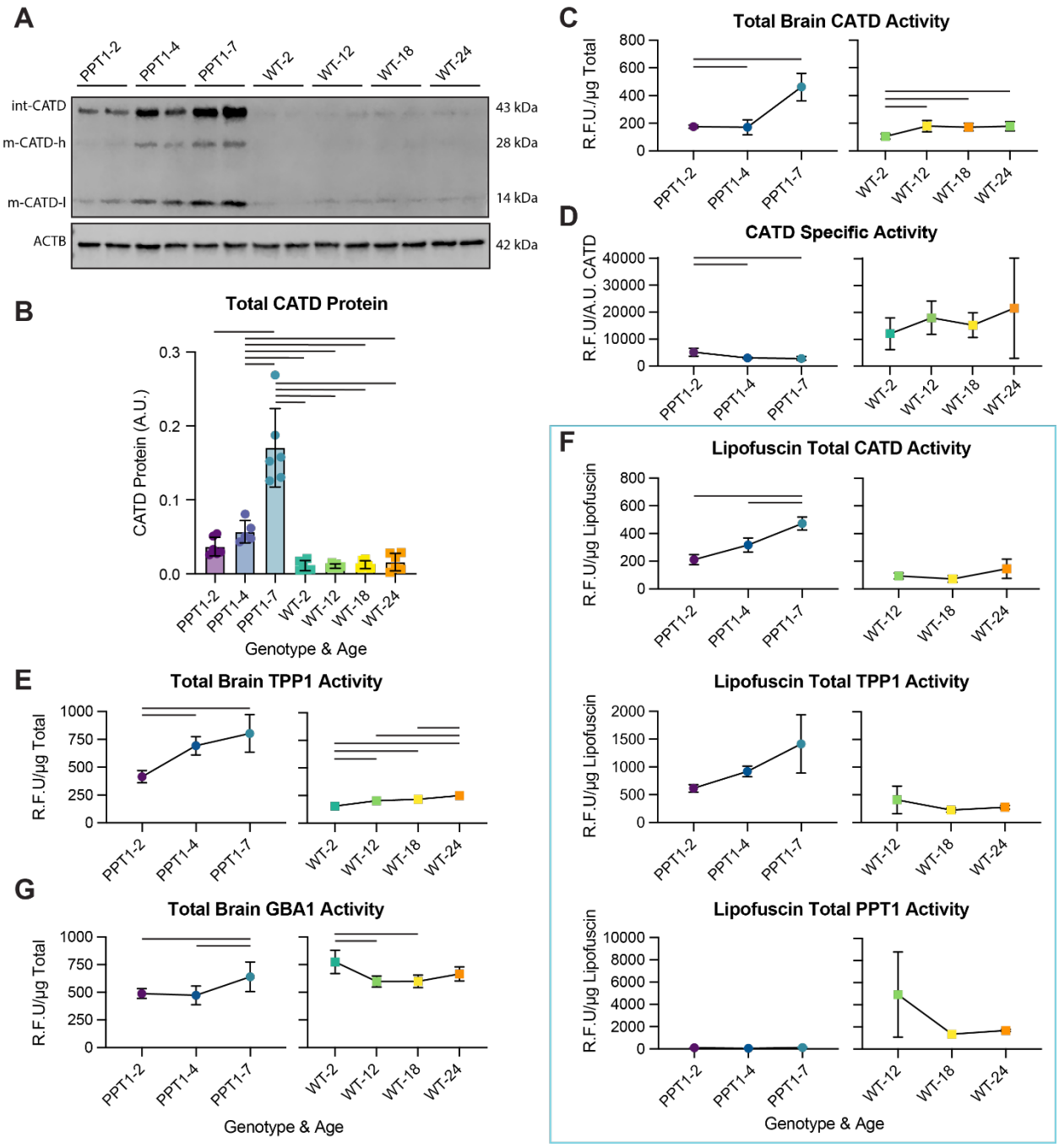
A
PPT1-2
PPT1-4
PPT1-7
WT-2
WT-12
WT-18
WT-24
int-CATD
m-CATD-h
m-CATD-I
ACTB
43 kDa
28 kDa
14 kDa
42 kDa
B
Total CATD Protein
CATD Protein (A.U.)
Genotype & Age
C
Total Brain CATD Activity
R.F.U./µg Total
D
CATD Specific Activity
R.F.U/A.U. CATD
E
Total Brain TPP1 Activity
R.F.U/µg Total
F
Lipofuscin Total CATD Activity
Lipofuscin Total TPP1 Activity
Lipofuscin Total PPT1 Activity
R.F.U/µg Lipofuscin
G
Total Brain GBA1 Activity
Genotype & Age

Figure S7. Levels and activity of enzymes implicated in lipofuscin biogenesis.

(**A**) Representative quantitative immunoblots of cathepsin D (CATD) across *CLN1* and aging conditions with actin (ACTB) loading control in total brain homogenates (n = 5-6 biological replicates/genotype/timepoint; int = intermediate; m = mature; h = heavy chain; l = light chain).

(**B**) Quantification of immunoblots of CATD protein in total brain homogenates (A.U.), normalized to actin loading control (n = 5-6 biological replicates/genotype/timepoint).

(**C**) Bulk CATD enzyme activity (R.F.U.) in total brain fractions normalized to total protein (μg) determined by BCA (n = 4-5 biological replicates/genotype/age).

(**D**) Specific enzyme activity of CATD (R.F.U./A.U. total CATD protein) in total brain homogenates (n = 4-5 biological replicates/genotype/age).

(**E**) Bulk TPP1 enzyme activity (R.F.U.) in total brain fractions normalized to total protein (μg) determined by BCA (n = 4-5 biological replicates/genotype/age).

(**F**) Bulk CATD, TPP1, and PPT1 enzyme activity (R.F.U.) in lipofuscin fractions (n = 3-5 biological replicates/genotype/age; n = 2 biological replicates for PPT1-4).

(**G**) Bulk GBA1 enzyme activity (R.F.U.) in total brain fractions normalized to total protein (μg) determined by BCA (n = 5-6 biological replicates/genotype/age).

Data are mean ± SD. Horizontal bars represent significant comparisons ($p < 0.05$) by 2-way ANOVA with Tukey's multiple comparisons test for immunoblot quantification and by one-way ANOVA with Tukey's multiple comparisons test for enzyme activity, throughout.

Fig. S8.

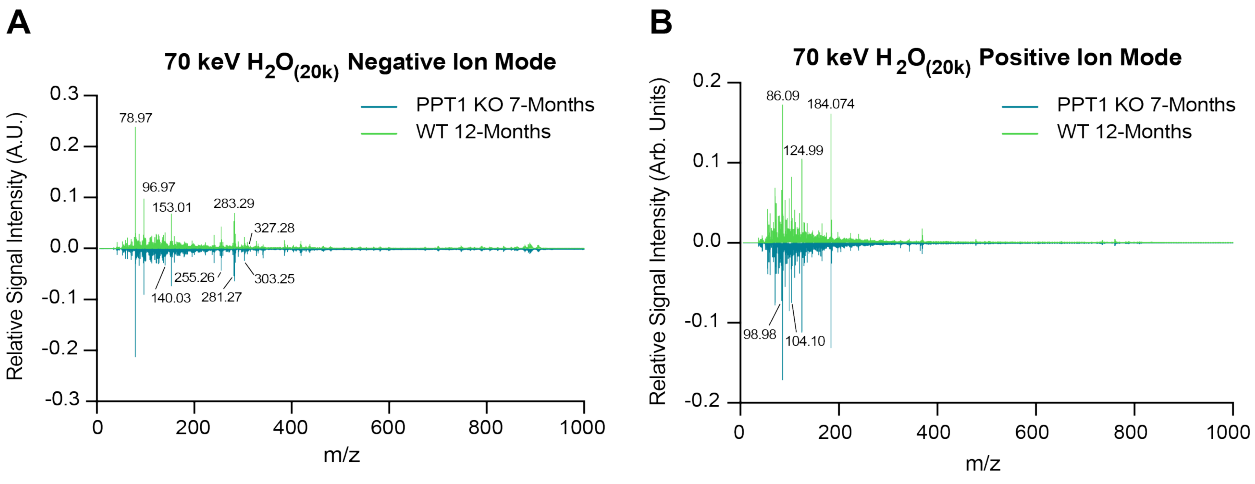
A
70 keV H2O(20k) Negative Ion Mode
PPT1 KO 7-Months
WT 12-Months
Relative Signal Intensity (A.U.)
m/z
78.97
96.97
153.01
283.29
327.28
255.26
303.25
140.03
281.27
B
70 keV H2O(20k) Positive Ion Mode
PPT1 KO 7-Months
WT 12-Months
Relative Signal Intensity (Arb. Units)
m/z
86.09
184.074
124.99
98.98
104.10

Figure S8. ToF-SIMS spectra of purified lipofuscin.

(**A-B**) ToF-SIMS spectra of purified lipofuscin from PPT1 KO 7-month and WT 12-month mice (average of $n = 3$ biological replicates) run using a 70 keV Gas Cluster Ion Beam (GCIB) in (A) negative ion mode and (B) positive ion mode with $(H_2O)_{20000}$ clusters with major peak mass-to-charge values (m/z) highlighted.

Fig. S9.

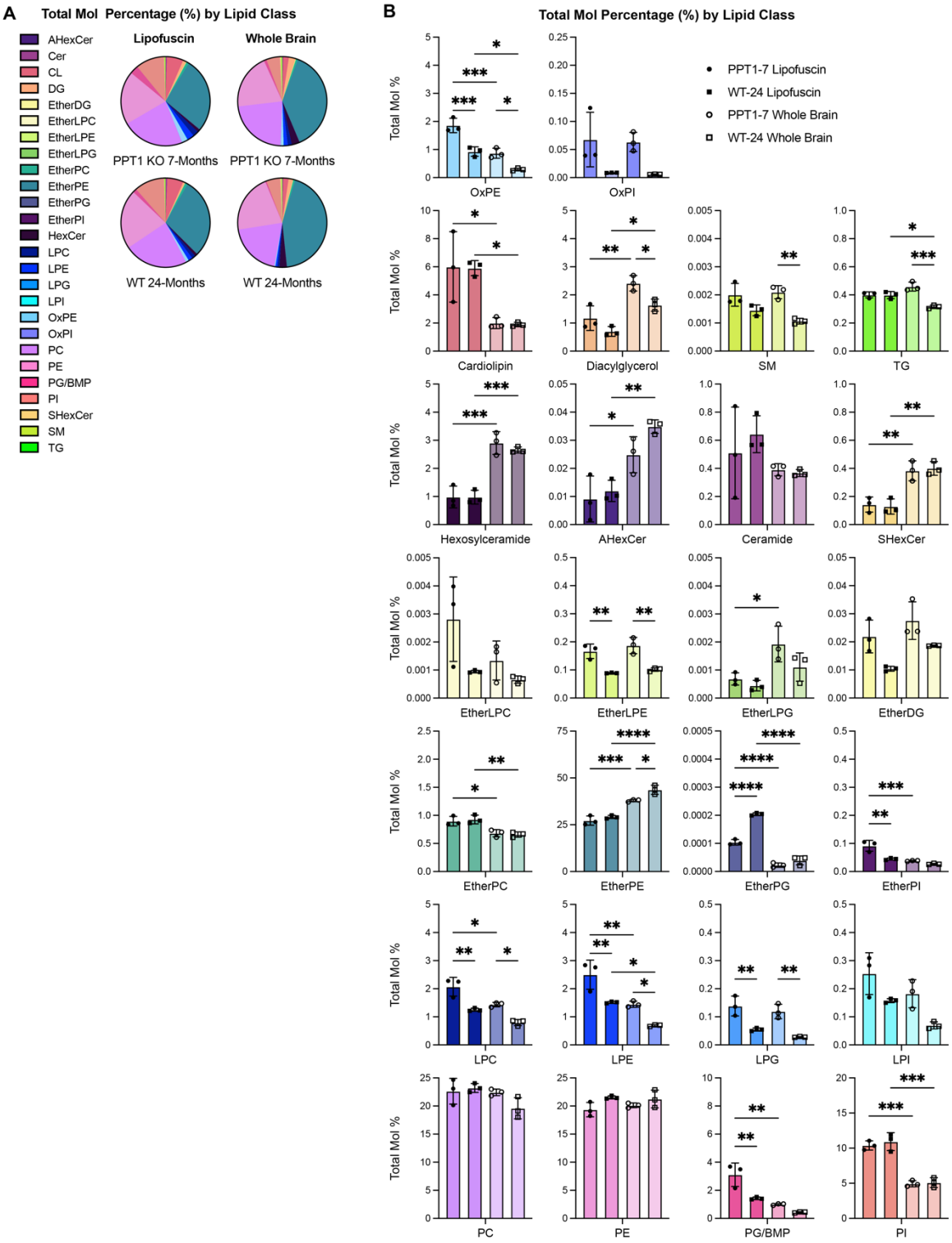
A
Total Mol Percentage (%) by Lipid Class
AHexCer
Cer
CL
DG
EtherDG
EtherLPC
EtherLPE
EtherLPG
EtherPC
EtherPE
EtherPG
EtherPI
HexCer
LPC
LPE
LPG
LPI
OxPE
OxPI
PC
PE
PG/BMP
PI
SHexCer
SM
TG
Lipofuscin
Whole Brain
PPT1 KO 7-Months
PPT1 KO 7-Months
WT 24-Months
WT 24-Months
B
Total Mol Percentage (%) by Lipid Class
PPT1-7 Lipofuscin
WT-24 Lipofuscin
PPT1-7 Whole Brain
WT-24 Whole Brain
Total Mol %
OxPE
OxPI
Cardiolipin
Diacylglycerol
SM
TG
Hexosylceramide
AHexCer
Ceramide
SHexCer
EtherLPC
EtherLPE
EtherLPG
EtherDG
EtherPC
EtherPE
EtherPG
EtherPI
LPC
LPE
LPG
LPI
PC
PE
PG/BMP
PI

Figure S9. Composition of lipofuscin and total brain by lipid class.

(**A**) Pie-charts of total mol % by lipid class for lipofuscin (left) and whole brain (right) for PPT1 KO 7-month samples (top) and WT 24-month samples (bottom). Statistical comparisons for each class are shown in adjacent bar graphs.

(**B**) Percent (%) contribution of lipid classes to total lipid content of lipofuscin and total brain from PPT1 7-month and WT 24-month mice. A-CAHexCer: acyl-hexosylceramide; Cer: ceramide; CL: cardiolipin; DG: diglyceride (diacylglycerol); EtherDG: ether-linked diglyceride; EtherLPC: ether-linked lysophosphatidylcholine; EtherLPE: ether-linked lysophosphatidylethanolamine; EtherLPG: ether-linked lysophosphatidylglycerol; EtherPC: ether-linked phosphatidylcholine; EtherPE: ether-linked phosphatidylethanolamine; EtherPG: ether-linked phosphatidylglycerol; EtherPI: ether-linked phosphatidylinositol; HexCer: hexosylceramide; LPC: lysophosphatidylcholine; LPE: lysophosphatidylethanolamine; LPG: lysophosphatidylglycerol; LPI: lysophosphatidylinositol; OxPE: oxidized phosphatidylethanolamine; OxPI: oxidized phosphatidylinositol; PC: phosphatidylcholine; PE: phosphatidylethanolamine; PG/BMP: phosphatidylglycerol/bis(monoacylglycero)phosphate; PI: phosphatidylinositol; SHexCer: sulfatide; SM: sphingomyelin; TG: triglyceride (triacylglycerol).

Data are mean ± SD. * $p < 0.05$, ** $p < 0.01$, *** $p < 0.001$ by one-way ANOVA with Tukey's multiple comparisons test.

Fig. S10.

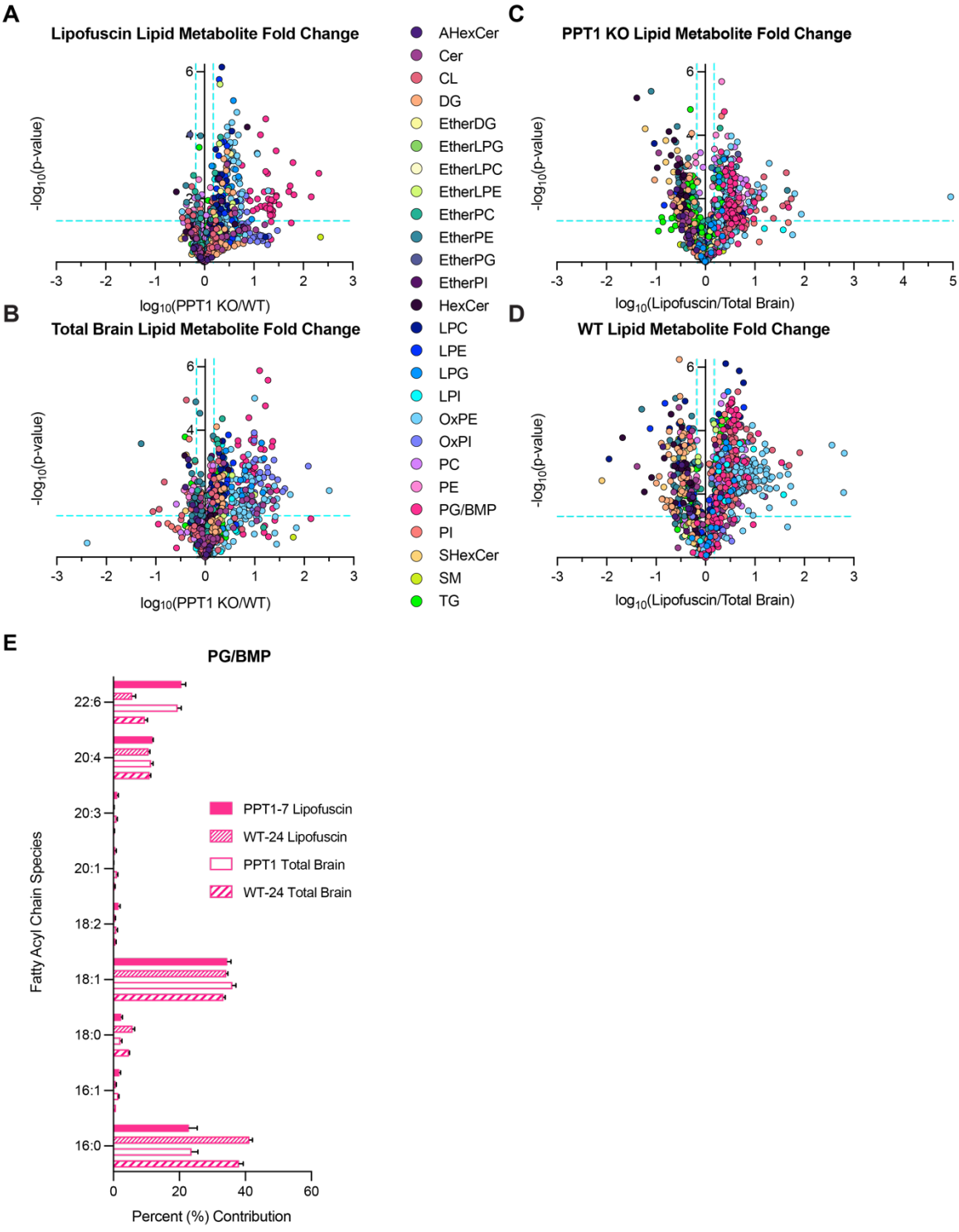
A
Lipofuscin Lipid Metabolite Fold Change
-log10(p-value)
log10(PPT1 KO/WT)
B
Total Brain Lipid Metabolite Fold Change
-log10(p-value)
log10(PPT1 KO/WT)
C
PPT1 KO Lipid Metabolite Fold Change
-log10(p-value)
log10(Lipofuscin/Total Brain)
D
WT Lipid Metabolite Fold Change
-log10(p-value)
log10(Lipofuscin/Total Brain)
AHexCer
Cer
CL
DG
EtherDG
EtherLPG
EtherLPC
EtherLPE
EtherPC
EtherPE
EtherPG
EtherPI
HexCer
LPC
LPE
LPG
LPI
OxPE
OxPI
PC
PE
PG/BMP
PI
SHexCer
SM
TG
E
PG/BMP
Fatty Acyl Chain Species
22:6
20:4
20:3
20:1
18:2
18:1
18:0
16:1
16:0
PPT1-7 Lipofuscin
WT-24 Lipofuscin
PPT1 Total Brain
WT-24 Total Brain
Percent (%) Contribution

Figure S10. Lipofuscin-enriched lipids and PG/BMP fatty acyl composition.

(**A-D**) Lipid metabolite fold-change comparisons between (A) WT 24-month and PPT1 KO 7-month lipofuscin, (B) WT 24-month and PPT1 KO 7-month total brain, (**C**) PPT1 KO 7-month lipofuscin and total brain, (D) WT 24-month lipofuscin and total brain. Colors represent lipid classes. Blue dashed lines indicate significant thresholds at 1.5-fold-change and $p = 0.05$ ($n = 3$ biological replicates/genotype). AHexCer: acyl-hexosylceramide; Cer: ceramide; CL: cardiolipin; DG: diglyceride (diacylglycerol); EtherDG: ether-linked diglyceride; EtherLPC: ether-linked lysophosphatidylcholine; EtherLPE: ether-linked lysophosphatidylethanolamine; EtherLPG: ether-linked lysophosphatidylglycerol; EtherPC: ether-linked phosphatidylcholine; EtherPE: ether-linked phosphatidylethanolamine; EtherPG: ether-linked phosphatidylglycerol; EtherPI: ether-linked phosphatidylinositol; HexCer: hexosylceramide; LPC: lysophosphatidylcholine; LPE: lysophosphatidylethanolamine; LPG: lysophosphatidylglycerol; LPI: lysophosphatidylinositol; OxPE: oxidized phosphatidylethanolamine; OxPI: oxidized phosphatidylinositol; PC: phosphatidylcholine; PE: phosphatidylethanolamine; PG/BMP: phosphatidylglycerol/bis(monoacylglycero)phosphate; PI: phosphatidylinositol; SHexCer: sulfatide; SM: sphingomyelin; TG: triglyceride (triacylglycerol).

(**E**) Percent (%) contribution (>1%) of fatty acyl chain species to PG/BMP isomer composition in PPT1 KO 7-month and WT 24-month lipofuscin and total brain ($n = 3$ biological replicates).